Nanoscale

Accepted Manuscript

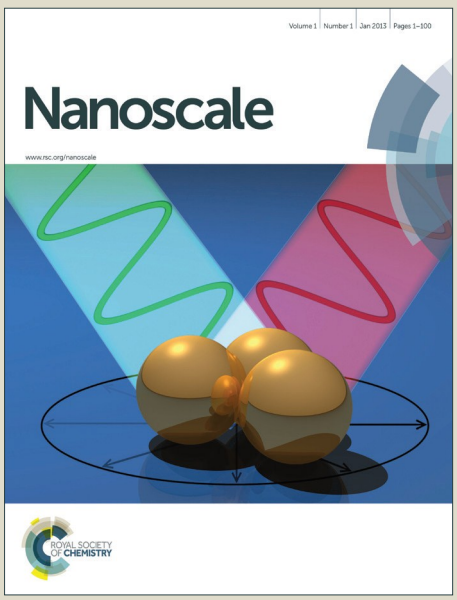

ROYAL SOCIETY OF CHEMISTRY

www.rsc.org/nanoscale

Nanoscale

Communication

Dielectric screening of excitons in monolayer Graphene

Premlata Yadav[a], Pawan Kumar Srivastava[a] and Subhasis Ghosh[a]*

Received 00th January 20xx,
Accepted 00th January 20xx

DOI: 10.1039/x0xx00000x

www.rsc.org/

Excitonic transitions in graphene monolayers embedded in different dielectric environment have been investigated using combined absorption and transmission spectroscopy. To vary the dielectric environment, graphene monolayer has been exfoliated in liquid medium. It has been shown that exciton binding energy decreases with increase in dielectric constant of exfoliating solvents due to screening of electron-electron and electron-hole interactions in graphene. The typical line shape of excitonic peak in absorption spectra is explained by Fano resonance between excitonic state and band continuum. Further it has been shown that, there exists a scaling relation between the dielectric constant of liquid and the exciton binding energy.

Introduction

Two dimensional (2D) materials such as graphene, have not only revealed a cornucopia of new physics, but also hold the potential to play a fundamental role in the future of nanoelectronic, optoelectronic and novel ultrathin, ultraflexible devices.[1-3] Many body interactions, such as excitonic effects (electron-hole interactions) are expected to play a significant role for 2D materials such as graphene, due to both the intrinsic enhancement of the importance of Coulomb interactions in 2D materials, as well as their reduced screening.[4-5] Compared with resonant excitons, bound electron-hole pairs are of peculiar interest because of their well-defined binding energy and much longer life time. Excitonic transitions in graphene occur at saddle point (M) of the Brillouin zone,[6] as shown in Fig. 1a. In contrast to excitonic transitions in other 2D systems, the line shape of excitonic peaks in graphene is asymmetric due to Fano resonances,[6-7] which results many body coupling between discrete excitonic state and the continuum states in the band descending from the saddle point. Further, there is a large scatter in the experimentally observed excitonic transition energy values reported in literature for samples prepared under different conditions, ranging from 4.5 eV for free standing graphene[6] to 4.96 eV for graphene on conducting substrates.[8] First principles calculations also predict excitonic peak positions varying from 4.1 eV to 5.2 eV depending on the strength of electron-electron (e-e) and electron-hole (e-h) interaction. [4,9,10] While the general features of excitonic transitions in graphene have been explored in some detail, the role of the dielectric environment, and associated screening effects have not been explored.

The investigation of exciton dielectric screening effects is non-trivial primarily due to the difficulties associated with discerning background screening effects. Incase of graphene, interaction effects are generally scaled by the fine structure constant, defined as the ratio of the average inter-electron coulomb interaction energy to the kinetic energy. Under Galilean invariance, the effective fine structure constant (α_G) which scales the strength of Coulomb interactions, is given *by* $\alpha_G = (n_0/n)^{1/2}$, where $n_0 = m^* e^2/\varepsilon\hbar^2$.[11] This implies that under Galilean invariance and within the framework of Fermi liquid description, the relative strength of many body effects in graphene is entirely controlled by the electron density. However, in monolayer graphene, due to the linear energy dispersion, the electrons at the Fermi energy are described in terms of an effective Lorentz invariant theory, wherein the fine structure constant (α_L) given by, $\alpha_L = e^2/\varepsilon\hbar v_F$, is independent of electron density and depends only on the material properties (v_F) and the dielectric environment (ε).[11-12] While it is unclear at this stage which description should be used to describe the properties of graphene.[5, 11-14] One way to avoid this unsettled issue is to work in a regime where the carrier concentration remains unchanged with changes in the dielectric environment.

In this letter, we present a systematic investigation on excitonic transitions in monolayer graphene in particular how the dielectric environment affects the excitonic transitions by screening the e-e and e-h interactions in graphene. Previous attempts to vary the dielectric environment, involved the use of different solid substrates.[6, 8, 15, 16] However, due to the incomplete immersion in dielectric medium, it is unclear if the exciton screening is partial or complete.[8, 14, 17] We vary the dielectric environment by exfoliating the graphene in a liquid medium, which allows us to tune the Coulomb interactions by choosing the liquids with different dielectric constant. We vary the dielectric constant, ε, from 2.4 to 37.5 using different polar and non-polar solvents, and show that there exists a scaling relation between the excitonic binding energy and the dielectric constant of the medium.

*Corresponding author email: subhasis@jnu.ac.in
[a]Electronic materials and Device Laboratory
School of Physical Sciences
Jawaharlal Nehru University
New Delhi-110067 (India)

Results and Discussion

We perform a liquid phase exfoliation to obtain monolayer graphene embedded in different dielectric environments[18]. This is a two step process which involves sonication of HOPG in organic solvents for 8-12 hours, followed by centrifugation of the sonicated solution in order to precipitate out thick graphitic flakes, as shown in Fig. 1b.

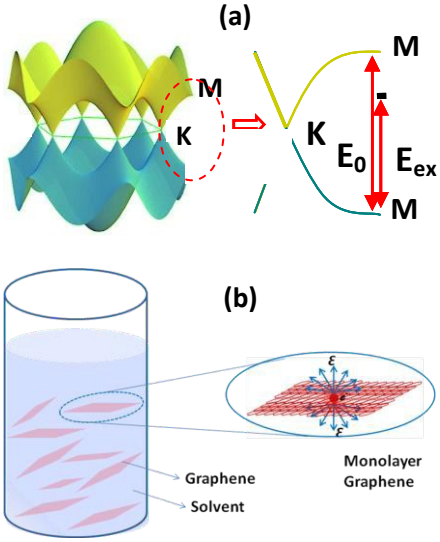

Fig. 1 Schematic representation of **(a)** the electronic band structure of graphene. The Dirac cones result a linear dispersion relation at the K points of the Brillouin zone. Excitonic transitions occurs at the M point i.e. saddle point. Excitonic states (E_{ex}) and the band edge energy (E_0) are shown by vertical lines **(b)** Monolayer graphene embedded in a solvent.

Fig. 2a shows the Raman spectra of different graphene samples exfoliated in toluene (ε = 2.4) and chlorobenzene (ε = 5.6). The pristine behavior of graphene is confirmed by the energetic position of the Raman G peak at 1580 cm^{-1}, the 2D peak at 2690 cm^{-1} and the absence of a D band.[19] We estimate the carrier concentration, n, from the blue shift of the G peak in Raman spectra using the relations, $n=[1/\pi(E_F/\hbar v_F)^2]$, and $E_F = (\omega_G - 1580)/42$ eV [20] where E_F and ω_G are the Fermi energy and the position of the G peak, respectively. Using these relations, n has been found to vary from 1.04 X 10^{11} cm^{-2} to 1.67 X10^{11} cm^{-2} as the dielectric constant of the solvents in which graphene is immersed was varied from 2.4 to 37.5, as shown in Fig. 2c.

Transfer characteristics from field effect transistors (FETs) also show the Dirac point (V_D) near zero gate bias for graphene prepared in toluene and chlorobenzene, as shown in Fig. 2b. The carrier concentration, *n*, has also been calculated using the relation, n= (C_g *V_D)/e,[21] where C_g is the gate capacitance. We measure C_g independently in each device instead of using the fixed value of C_g = 11.5 nF/cm^2 for 300 nm of SiO_2, which may lead to incorrect interpretation of the data. The carrier concentration extracted from FET characteristics varies from 2.1 x 10^{11} cm^{-2} to 3.7 x 10^{11} cm^{-2}, as shown in Fig. 2c.

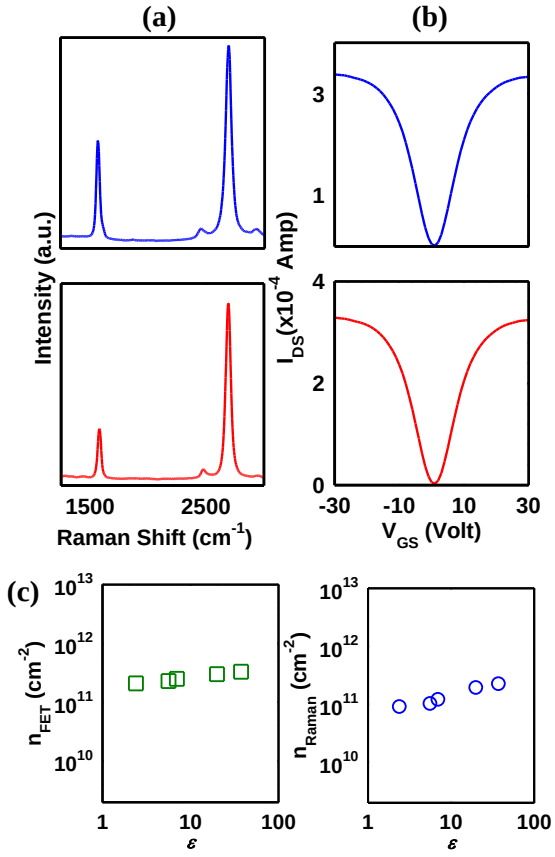

Fig. 2 (a) Raman spectra of monolayer graphene exfoliated in toluene (top) and chlorobenzene (bottom). In each case, Raman G and 2D peak position were observed at 1580 cm^{-1} and 2690 cm^{-1} respectively. D peak is absent for both graphene layers indicating negligible defect density and Dirac point close to zero gate bias show pristine behaviour of graphene. **(b)** Transfer characteristics of monoloyer graphene FETs exfoliated in toluene (top) and chlorobenzene (bottom). **(c)** Carrier concentration, n_{FET} and n_{Raman} determined from the transfer characteristics of graphene based FETs and Raman measurements, respectively.

To substantiate the screening effect on the excitons in monolayer graphene by the external dielectric environment, it is required to exclude other possible factors that may also influence the optical transition energies, including strain, [22] doping or charge transfer.[23, 24] It is known that Raman spectra are sensitive to such external perturbations in graphene.[19, 25, 26] We observe no shifts or changes in the peak shape from the Raman spectra, and the intensity ratios from the Raman spectra I_G/I_{2D} for various samples falls within the range 0.3 ± 0.05 (Fig. 3), consistent with the expectation for high quality graphene monolayers.[19, 26] It is argued that, presence of lattice defects/external perturbation in graphene monolayers will result in lattice expansion/contraction, which consequently results in to stiffening/softening of the phonons.[2] This phenomenon should be primarily reflected in the shift in Raman G and 2D modes of graphene[22]. We have thoroughly examined the relative shift in various graphene monolayers samples prepared in different solvents. as discussed earlier, position of G and 2D peak falls near ~1580 cm^{-1} and ~2690 cm^{-1} for graphene prepared in different chosen solvents (Fig. 3). This rule out the

possibility of strong phonon interactions and its considerable effect on excitonic transitions. Chemical reactions would favour covalent functionalization of graphene monolayers resulting in lattice defects which should be reflected as substantial Raman D peak intensity. Interestingly, no substantial D peak intensity has been observed in any of graphene samples. Moreover, any chemical reaction will induce charge transfer resulting *p*-type or *n*-type doping in graphene layers. As a consequence, V_D should shift to positive or negative gate bias[21]. We have not observed significant shift in position of the V_D in devices based on graphene monolayers prepared in different solvents. V_D in several graphene monolayers based devices has been consistently observed near zero gate bias. From these observations, we have been able to rule out the effect of phonon interactions and charge transfer between graphene and the solvent molecules.

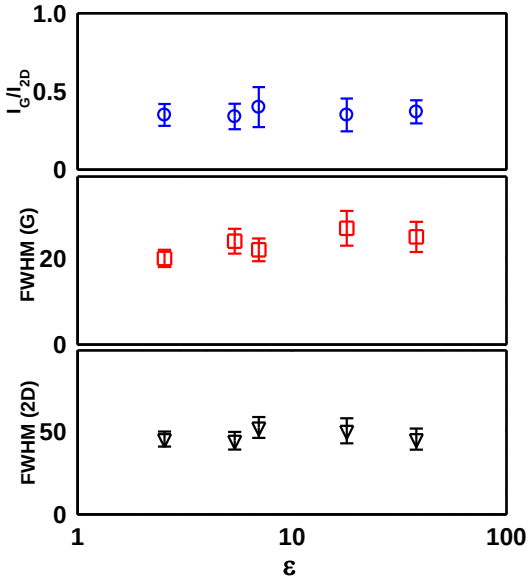

Fig. 3 Intensity ratio of Raman G to 2D peaks (I_G/I_{2D}) and full width half maximum of G, FWHM (G) and 2D peaks, FWHM (2D) as a function of respective dielectric constants. Errors bars signify variation in measured parameters on 10 different graphene monolayers.

Fig. 4a and b show the optical absorption spectra of monoloyer graphene exfoliated in toluene (ε~ 2.4) and acetone (ε~ 17.7), respectively. The absorption data were collected from graphene immersed in the solvent in which it was prepared. We find that the absorbance starts increasing non-monotonically from 2.5 eV, and excitonic peaks are seen at 4.33 eV and at 4.60 eV. We find that the excitonic peak shifts to higher energy with increasing dielectric constant. The blue shift in the peak position of exciton is expected to be entirely controlled by the dielectric environment, as it has already been shown that carrier concentration remains relatively constant. In case of graphene immersed in solvent with low dielectric environment, dielectric screening is weak and leads to strong Coulombic interactions (e-e interactions), while dielectric screening is more for high dielectric environment leading to reduced e-e interactions. Effect of dielectric screening on shift in excitonic peak positions will be discussed later. The line shapes are found to be asymmetric and the degree of asymmetry reduces substantially with increasing dielectric constant.

The exciton binding energy (E_b), is given by E_0-E_{ex}, where E_0 the electronic band gap at the M point, and E_{ex} is the exciton energ or excitonic peak position. The asymmetric line shape of th absorption spectra can be interpreted as a consequence of F n resonance, resulting from the coupling between the continuu electronic state near the M point and the discrete excitonic state The line shape can be fitted using the Fano model, [6,7] with A_{Fa} $=A[(p+q_F)^2/(1+q_F)^2]$, where A is an overall scaling factor. The Fano parameter for asymmetry, q_F, is given by, $q_F=E_0-E_{ex}/(\Gamma/2)$, and Γ the width of discrete state, and $p = (E-E_{ex})/(\Gamma/2)$.[7] The fits are show as solid lines in Fig. 4. The fitting parameters are q_F = -8.57, Γ = 0.26 eV, E_{ex} = 4.38 eV, E_0 = 5.06eV and q_F = -6.6, Γ = 0.17 eV, E_{ex} = 4.62 eV, E_0 = 5.10 eV for graphene monolayers exfoliated and immerse in dielectric environment with ε = 2.4, and ε = 17.7, respectively The change in the value of q_F can be accounted due to change line shape of the absorption spectra. Higher/lower values of signify the strong/weak interaction of electrons with continuum state. In our case, we have obtained q_F ~ -8.57 and -6.6 graphene prepared in toluene and acetone, respectively. It indicates that electron interaction with continuum is relati stronger in case of graphene prepared in toluene owing to smalle dielectric constant of toluene (less dielectric screening) leading t more asymmetry in the absorption line shape. In contrast, electro interaction with continuum would be effectively screened in cas graphene prepared in acetone due to higher dielectric constant o acetone (higher dielectric screening) and hence less asymmetry ha been observed in the absorption line shape.

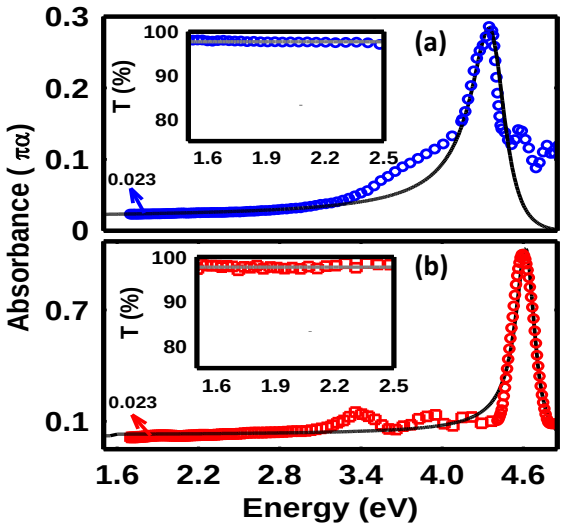

Fig. 4 Optical absorption and transmittance spectra of graphene monolayers exfoliated in **(a)** toluene (ε =2.4) and **(b)** acetone (ε =17.7 , with excitonic peaks at 4.34 eV and 4.6 eV respectively. The line shapes fo excitonic peaks are asymmetric, with a larger asymmetry associated wit higher dielectric constant. The lineshapes are understood using Fano mode and solid lines show fits using the Fano model. Insets shows transmittance data of graphene sample in the energy range 1.5 eV to 2.5 eV. The solid li corresponds to the theoretical value of universal transmittance, i.e. 97.7 % as that for monolayer graphene.

Despite being only one atom thick, graphene has been found to absorb a significant fraction of the incident light, a consequence of graphene's unique electronic structure.[27] The transmittance of graphene layer is defined by T = (1 - Nπα), where N is the number of graphene layers.[28] According to this relation, monolayer graphene absorbs a fraction of incident light πα (~ 2.3%) and hence should show a universal transmittance of ~ 97.7 %. The transmittance spectra acquired in the energy range 1.5 eV to 2.5 eV for exfoliated graphene monolayers for low ε (toluene) and high ε (acetone) solvents are shown in the insets of Fig. 4a and b, consistent with the expected transmittance relation. We find that the optical transmittance is independent of the dielectric environment and shows deviation from universality only at higher energies.

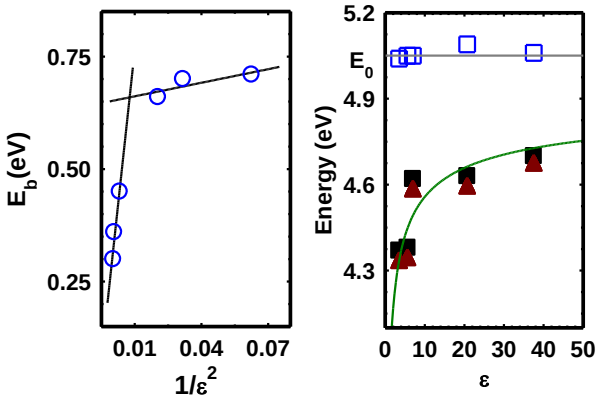

Fig. 5 **(a)** The binding energy of the exciton, E_b, as a function of ε. It can be seen that E_b does not vary linearly with $1/\varepsilon^2$. **(b)** Experimentally and phenomenologically obtained exciton energies and band edge energies (empty square markers) calculated from Fano fitting as a function of ε. Solid line represents fit to the excitonic energies determined from UV-visible absorption (solid triangle) and from the Fano fitting (solid square), with x = 1.2. The peak positions are blue shifted with increase in value of ε is an indication of screening or reduced e-e interactions in case of graphene exfoliated in high dielectric medium. The value of E_0 obtained from fitting using expression for exciton binding energy is 5.04 eV which is close to the values (5.04 eV ≤ E_0 ≤ 5.10 eV) obtained from Fano fitting. Solid horizontal line represents average value of E_0 = 5.04 eV.

Fig. 5a shows the variation in E_b as a function of ε. It is clear that E_b does not vary linearly with $1/\varepsilon^2$ as in the case of three-dimensional and quasi-2D systems.[29] However, shift in excitonic peak positions can be explained using Fig. 5a. Especially, in high-k solvents due to small E_b, excitonic peak will shift to higher energy (since $E_b = E_0 - E_{ex}$) as observed in our case (Fig. 4b). With increase in surrounding dielectric environment, *e-e* or *e-h* interaction reduces due to increased dielectric screening (low E_b) resulting blue shift in the excitonic peak position. So the blue shift of exciton peak as observed in case of graphene monolayers prepared in acetone (k~17.7) is an indication of screening or reduced *e-e* interactions. In case of graphene immersed in low dielectric environment (in toluene, k~2.4), relatively weak dielectric screening leads to strong Coulombic interactions (large E_b) and excitonic peak is relatively red shifted as compared to that of graphene prepared in acetone. We calculate the effective mass, m^*, from straight line fits to the data, as represented by the solid lines. Elias et al.[5] have reported the measurement of the cyclotron mass in suspended graphene for n varying over three orders of magnitude. From the steeper slope, we extract $m^* = 0.042\ m_0$, where m_e is the free electron mass, in close agreement to previously reported values.[5] The extrapolated value for the binding energy as ε approaches infinity is estimated to be 0.31 eV. The effective mass calculated from the second slope is 0.0009 m_0, approximately two orders of magnitude smaller than the previous value. As discussed before, similar n has been obtained for all graphene samples. Hence, this variation in m^* cannot be explained on the basis of variation in n and ε. The binding energy estimate for E_b for $\varepsilon = \infty$ is 0.65 eV. In order to reconcile the different observations, we introduce a scaling of the binding energy, E_b. Fig. 5b shows the variation in E_0 and E_{ex}, determined from the Fano fitting and the absorption spectra, respectively, as a function of ε. The relation between E_b and ε shows power law dependence and accordingly, the exciton binding energy is given by $E_{ex} = E_0 - m^* e^4/2h^2\varepsilon^x$. By fitting the experimental data with this expression, we extract, x = 1.2. From the intercept of the fitted curve, the value of E_0 has been found to be 5.04 eV, which is fairly close to the values obtained for the excitonic peaks, from the Fano model.

Conclusions

In summary, we have resolved the ambiguity in excitonic peak position revealing the role of the Coulomb interactions in monolayer graphene, via a unique method by which dielectric environment of immersed graphene is varied to modulate the Coulombic interaction. There is a strong shift in excitonic peak position with change in dielectric environment of graphene due to screening of Coulombic interactions. It has been shown that the Fano model describes the line shape of the absorption spectra of excitonic transitions. The degree of asymmetry varies with dielectric environment and hence with Coulombic interaction in graphene. There is a scaling relation between E_b and ε^x, with x =1.2 which needs to be further established by detailed theoretical investigations. It is known that optical and electronic properties of single walled carbon nanotubes (SWCNTs) dominated by Coulomb interactions and exciton binding energy is strongly dependent on screening of Coulomb interactions under various dielectric environments. In case of SWCNTs, it has been shown that there is a scaling relation between E_b and ε_x, where x is not 2, but varies from 1 to 1.4.[30] Similar scaling of E_b with ε suggests that screening of Coulomb interactions in different dielectric environment plays crucial role in case of graphene monolayer.

Acknowledgement

Authors thank WITec GmbH, Germany for his help in Raman spectroscopic measurements. We thank Dr. Nirat Ray for valuable discussion. P. Yadav and P. K. Srivastava thanks UGC and CSIR, India for financial assistance through fellowship.

References

1. A. K. Geim and K. S. Novoselov, *Nat. Mater*. 2007, **6**, 183.
2. K. Novoselov, D. Jiang, F. Schedin, T. Booth, V. Khotkevich, S.Morozov, and A. Geim, *Proceedings of the National Academy of Sciences of the United States of America* 2005, **102**, 10451.
3. K. S. Novoselov, V. Fal, L. Colombo, P. Gellert, M. Schwab, K. Kim, *Nature* 2012, **490**, 192.
4. K. F. Mak, J. Shan, and T. F. Heinz, *Phys. Rev. Lett*. 2011, **106**, 046401.
5. D. C. Elias, R. V. Gorbachev, A. S. Mayorov, S. V. Morozov, A. A. Zhukov, P. Blake, L. A. Ponomarenko, I. V. Grigorieva, K. S. Novoselov, F. Guinea and A. K. Geim, *Nat. Phys*. 2011, **7**, 701.
6. D.-H. Chae, T. Utikal, S. Weisenburger, H. Giessen, K. v. Klitzing, M. Lippitz, and J. Smet, *Nano Lett.* 2011, **11**, 1379.
7. T.-T. Tang, Y. Zhang, C.-H. Park, B. Geng, C. Girit, Z. Hao, M. C. Martin, A. Zettl, M. F. Crommie, S. G. Louie, et al., *Nat, Nanotech.* 2010, **5**, 32.
8. I. Santoso, P. K. Gogoi, H. B. Su, H. Huang, Y. Lu, D. Qi, W. Chen, M. A. Majidi, Y. P. Feng, A. T. S. Wee, K. P. Loh, T. Venkatesan, R. P. Saichu, A. Goos, A. Kotlov, M. R¨ubhausen, and A. Rusydi, *Phys. Rev. B* 2011, **84**, 081403.
9. L. Yang, J. Deslippe, C.-H. Park, M. L. Cohen, and S. G. Louie, *Phys. Rev. Lett.* 2009, **103**, 186802.
10. L. Yang, M. L. Cohen, and S. G. Louie, *Nano Lett.* 2007, 7, 3112.
11. V. N. Kotov, B. Uchoa, V. M. Pereira, F. Guinea, and A. H. Castro Neto, *Rev. Mod. Phys.* 2012, **84**, 1067.
12. S. Das Sarma, S. Adam, E. H. Hwang, and E. Rossi, *Rev. Mod. Phys.* 2011, **83**, 407.
13. S. Das Sarma, E. H. Hwang, and W.-K. Tse, *Phys. Rev. B* 2007, **75**, 121406.
14. C. Hwang, D. A. Siegel, S.-K. Mo, W. Regan, A. Ismach, Y. Zhang, A. Zettl, and A. Lanzara, *Sci. Rep.* 2012, **2**, 590.
15. V. G. Kravets, A. N. Grigorenko, R. R. Nair, P. Blake, S. Anissimova, K. S. Novoselov, and A. K. Geim, *Phys. Rev. B* 2010, **81**, 155413.
16. I. Santoso, R. S. Singh, P. K. Gogoi, T. C. Asmara, D. Wei, W. Chen, A. T. S. Wee, V. M. Pereira, and A. Rusydi, *Phys. Rev. B* 2014, **89**, 075134.
17. W. Sheng, M. Sun, A. Zhou, and S. J. Xu, *Appl. Phys. Lett.* 201[illegible], **103**, 143109.
18. P. K. Srivastava, P. Yadav and S. Ghosh, *RSC Adv.,* 2015, [illegible] 64395.
19. A. C. Ferrari, *Solid State Commun.* 2007, **143**, 47.
20. H. Yan, F. Xia, W. Zhu, M. Freitag, C. Dimitrakopoulos, A. A. Bo[illegible] G. Tulevski, and P. Avouris, *ACS Nano* 2011, **5**, 9854.
21. J. Yan, Y. Zhang, P. Kim, and A. Pinczuk, *Phys. Rev. Lett.* 2007, **98**, 166802.
22. S. B. Cronin, A. K. Swan, M. S. Unlu, B. B. Goldberg, M. S. Dresselhaus, and M. Tinkham, *Phys. Rev. B* 2005, **72**, 035425.
23. M. Shim, A. Javey, N. W. Shi Kam, and H. Dai, *J. Am. Chem. [illegible]* 2001, **123**, 11512.
24. A. Zahab, L. Spina, P. Poncharal, and C. Marli`ere, *Phys. Rev. B* 2000, **62**, 10000.
25. A. C. Ferrari, J. C. Meyer, V. Scardaci, C. Casiraghi, M. Lazzeri, F. Mauri, S. Piscanec, D. Jiang, K. S. Novoselov, S. Roth, and A. K. Geim, *Phys. Rev. Lett.* 2006, **97**, 187401.
26. C. Casiraghi, S. Pisana, K. S. Novoselov, A. K. Geim, and A. C Ferrari, *Appl. Phys. Lett.* 2007, **91**, 233108.
27. A. Tiberj, M. Rubio-Roy, M. Paillet, J.-R. Huntzinger, P. Landois, M. Mikolasek, S. Contreras, J.-L. Sauvajol, E. Dujardin, and A.-A. Zahab, *Sci. Rep.* 2013, **3**, 2355.
28. R. Nair, P. Blake, A. Grigorenko, K. Novoselov, T. Booth, T Stauber, N. Peres, and A. Geim, *Science* 2008, **320**, 1308.
29. W. Langbein and J.M. Hvam *Phys. stat. sol. (b)* 1998, **206**, 111
30. V. Perebeinos, J. Tersoff, and P. Avouris, *Phys. Rev. Lett.* 2004, **92**, 257402.